

Knockdown of EFEMP1 Promotes Ferroptosis by Inactivating PI3K/AKT to overcome the Resistance of Hepatocellular Carcinoma Cells to Sorafenib

Ti Zhou, Haibin Lan, Yao Ma, Donglin Fang

Department of General
Surgery, The First People's
Hospital of Linping District,
Hangzhou, China

Address for correspondence:

Donglin Fang

Department of General
Surgery, The First People's
Hospital of Linping District,
Hangzhou, 369 Yingbin Road,
Liping District, Hangzhou
City, Zhejiang Province, China
fangdl069@163.com

ABSTRACT

Background & Aims: We found epidermal growth factor-containing fibulin-like extracellular matrix protein 1 (EFEMP1) is up-regulated in liver cancer cells exposed to sorafenib for a long time using a bioinformatic tool. Here, the mechanism of EFEMP1 in sorafenib resistance of hepatocellular carcinoma (HCC) cells was explored.

Methods: Human HCC cell lines Huh7 and HCCLM3 received low concentrations of sorafenib for a long time to construct sorafenib-resistant Huh7 and HCCLM3 (Huh7-SR and HCCLM3-SR) cells. HCCLM3, HCCLM3-SR, Huh7 and Huh7-SR cells received sorafenib, and the cell viability was assayed by CCK-8 method. HCCLM3-SR and Huh7-SR cells were transfected before sorafenib treatment, and these cells apoptosis was determined with flow cytometry assay. Ferroptosis-related index, EFEMP1, phosphorylated PI3K (p-PI3K), p-AKT level in HCCLM3, HCCLM3-SR, Huh7 and Huh7-SR cells was detected using flow cytometry assay, colorimetry, qRT-PCR and Western blot analysis, respectively.

Results: Following sorafenib treatment, HCCLM3-SR (8/16 μ M) and Huh7-SR (4/8/16/32 μ M) cell viability was higher than HCCLM3 and Huh7 cell viability. HCCLM3-SR and Huh7-SR cells presented higher IC₅₀ of sorafenib. Following sorafenib (7 μ M) treatment, ROS, MDA, TBARS, Fe²⁺ level in HCCLM3-SR and Huh7-SR cells was lower, and SLC7A11, GPX4, EFEMP1, p-AKT and p-PI3K level in Huh7-SR and HCCLM3-SR cells was higher than those in HCCLM3 and Huh7 cells. Under sorafenib (7 μ M) treatment, EFEMP1 silencing promoted apoptosis, up-regulated ROS, MDA, TBARS, Fe²⁺ level and inhibited SLC7A11, GPX4, p-AKT and p-PI3K expression in Huh7-SR and HCCLM3-SR cells.

Conclusions: Knockdown of EFEMP1 promotes ferroptosis by inactivating PI3K/AKT to resensitize sorafenib-resistant HCC cells to sorafenib.

Key words: EFEMP1 – sorafenib – PI3K/AKT – hepatocellular carcinoma – ferroptosis.

Abbreviations: AKT: protein-serine-threonine kinase; CCK-8: cell counting kit-8; EFEMP1: epidermal growth factor-containing fibulin-like extracellular matrix protein 1; GEO: Gene Expression Omnibus; HCC: hepatocellular carcinoma; IC: inhibitory concentration; MAO: malondialdehyde; mTOR: mechanistic target of rapamycin; PI3K: phosphoinositide 3-kinase; ROS: reactive oxygen species; TBARS: thiobarbituric acid reactive substances; TKI: tyrosine kinase inhibitor.

INTRODUCTION

Liver cancer is a main reason for tumor-associated mortality among patients, and hepatocellular carcinoma (HCC) represents 75%-85% of cases with primary liver cancers [1, 2]. Surgical excision is the first-choice therapeutic strategy for HCC rather than for patients suffering from advanced, metastatic HCC

[3], which yet predicts poor clinical outcomes, with an average five-year survival rate as low as 2.5% in US [4]. For these advance-staged HCC, systemic therapy with tyrosine kinase inhibitors (TKIs) emerges as a dominant option [4].

Sorafenib, which is a multiple-targeted TKI, has been considered for a decade to be the first line and standard targeted therapy for advanced HCC [2, 5]. Sorafenib inhibits cancer cell proliferation via repressing Raf-1, B-Raf, and kinase activity [6]. Previous trials on the anti-tumor efficacy of sorafenib in HCC showed an around 3-month extension in the median overall survival of patients suffering from advanced HCC. However, few patients develop the acquired resistance of sorafenib

Received: 20.08.2025

Accepted: 20.02.2026

within 6 months of treatment, which prevents them benefiting from sorafenib treatment [6, 7]. Hence, the identification of the critical issues related to sorafenib resistance is of great importance to HCC treatment.

Ferroptosis is a type of regulated non-apoptotic, iron-dependent cell death, featuring overwhelming lipid peroxidation caused by iron accumulation and reactive oxygen species (ROS) overproduction [8]. Up-regulation of ferroptosis augments the anti-cancer effect of sorafenib on HCC [9], while ferroptosis inhibition drives resistance to Sorafenib [10]. Here, using Gene Expression Omnibus (GEO) data package GSE62813, we obtained genes whose expression changes in liver cancer cells after a long-term exposure to sorafenib, and then screened out genes showing significant differences in the expression from them with a conditional filter of $|\log_{2}FC| > 6$. Further, by taking the intersection of the screened-out genes that are up-regulated in sorafenib and sorafenib-withdrawal groups in comparison with those in the control group, 12 candidate genes were obtained. Finally, through overlapping them with the ferroptosis-related genes in literatures [11], we targeted epidermal growth factor-containing fibulin-like extracellular matrix protein 1 (EFEMP1) as our research object. EFEMP1, alternatively known as Fibulin-3, belongs to the fibulin glycoprotein family, and has a role in the stabilization of the basement membrane and the maintenance of the extracellular matrix structure [12, 13]. It is also involved in cancer development and progression by functioning cancer type-dependently as a tumour promote or suppressor [14] as well as impacting on the resistance of cancer cells to some drugs [15]. In HCC, it represses cancer cell growth and migration [16, 17], and its downregulation indicates poor prognosis [18]. Data package analysis showed that long-term exposure to sorafenib could up-regulate EFEMP1 in liver cancer cells. Nevertheless, how EFEMP1 affects sorafenib-resistant HCC cells is unclear. A recent study reported that EFEMP1 associates with the inhibition of ferroptosis in endometriosis [11]. Although EFEMP1 seems to be a tumor suppressor in HCC, since preventing ferroptosis augments the resistance to sorafenib, EFEMP1 may conduce to the sorafenib resistance in sorafenib-resistant HCC by inhibiting ferroptosis.

The phosphoinositide 3-kinase (PI3K)/protein-serine-threonine kinase (AKT) pathway is a main downstream signaling pathway contributing to tumor cell metastasis, invasion and migration [19, 20]. PI3K/AKT pathway activation in HCC promotes metastasis and invasion [21], and causes resistance to sorafenib, and more pertinently, it decreases the sensitivity of sorafenib-resistant HCC cells to sorafenib by repressing sorafenib-induced ferroptosis [22]. EFEMP1 activates the PI3K/AKT pathway in pleural mesothelioma [19]. In this case, we speculate EFEMP1 inhibits ferroptosis via activating PI3K/AKT to augment sorafenib resistance of HCC cells.

Here, ferroptosis and the expressions of EFEMP1 and the PI3K/AKT pathway in sorafenib-sensitive and sorafenib-resistant HCC cells were compared. Furthermore, how EFEMP1 affects ferroptosis via mediating PI3K/AKT axis to regulate sorafenib resistance of HCC cells was studied.

METHODS

Cell culture and treatment

Human HCC cell lines HCCLM3 (CL-0278) and Huh7 (CL-0120) were obtained from Procell (Wuhan, China) and cultured in special media for HCCLM3 or Huh7 cells (CM-0278; CM-0120, Procell, Wuhan, China) at 37°C with 5% CO₂. Sorafenib (C₂₁H₁₆ClF₃N₄O₃, 99.88%, HY-10201, MedChemExpress, Monmouth Junction, New Jersey, USA) was dissolved in dimethyl sulfoxide (DMSO, abs9184, absin, Shanghai, China) and diluted in culture medium. HCCLM3 and Huh7 cells received increasing concentrations (3, 5 and 7 μM) of sorafenib for 3 months (1 month for each concentration) to construct sorafenib-resistant HCCLM3 and Huh7 (HCCLM3-SR and Huh7-SR) cells [23]. HCCLM3, HCCLM3-SR, Huh7 and Huh7-SR cells received sorafenib at 0, 4, 8, 16 or 32 μM for 24 h to assess the role of different concentrations of sorafenib in HCCLM3-SR and Huh7-SR cells using Cell Counting Kit-8 (CCK-8) assay [22]. In other experiments, HCCLM3, HCCLM3-SR, Huh7 and Huh7-SR cells were treated for 24 h with or without sorafenib at 7 μM [22, 24].

CCK-8 Assay

HCCLM3, HCCLM3-SR, Huh7 and Huh7-SR cell viability was determined with a CCK-8 kit (GK10001, GLPBIO, Shanghai, China). Specifically, cells at 1×10⁴ cells/well were incubated in a 96-well plate (CLS3922, Sigma-Aldrich, Saint Louis, Missouri, USA) in 100 μL medium. Cells were subjected to 24-h incubation at 37°C with 5% CO₂. After exposure to sorafenib at 0, 4, 8, 16 or 32 μM for 24 h, CCK-8 solution (10 μL) was added into each well, followed by 4-h incubation. After gentle mixing for 1 min, the absorbance at 450 nm was measured using a microplate reader (1215D29, Thomas Scientific, Swedesboro, New Jersey, USA). Graphpad 8.0 software (Graphpad Software, San Diego, California, USA) was employed to calculate the half-maximal drug inhibitory concentration (IC₅₀).

Cell Transfection

Cell transfection was conducted before sorafenib treatment. Short hairpin RNA against EFEMP1 (shEFEMP1, Target Seq: 5'-CCAGTCAATAGTCTACAAATA-3') and short hairpin RNA negative control (shNC, C03002) were designed and synthesized by Genepharma (Shanghai, China). HCCLM3-SR and Huh7-SR cells at about 80% confluence were transfected with shEFEMP1 or shNC using Lipofectamine™ 3000 (L3000150, Thermo Fisher, Waltham, Massachusetts, USA) for 48 h at 37°C.

Quantitative Real Time Polymerase Chain Reaction (qRT-PCR)

Total RNA was isolated from HCCLM3-SR and Huh7-SR cells using the RNA extraction kit (R1200, Solarbio, Beijing, China). The total RNA was quantified using an UV spectrophotometer (DR6000, HACH, Shanghai, China). Total RNA was then reverse transcribed using a Primescript™ RT reagent Kit (DRR041A, 3-biologic, Shanghai, China). qRT-PCR was performed using the SYBR Premix Ex Taq II

(RR820A, TaKaRa, Osaka, Japan) in a StepOne Plus real-time PCR system (114469, HUANXIYL, Shanghai, China). The qRT-PCR amplification program was as follows: 5 min at 95°C; 10 s at 95°C, 20 s at 60°C and 20 s at 72°C for 45 cycles and 10 min at 72°C. Gene expression level was analyzed with the $2^{-\Delta\Delta Ct}$ method [25], and expression of GAPDH served as the inner standard. Primers are presented as follows: EFEMP1, forward: 5'-GTCACAGGACACCGAAGAAAC-3' and reverse: 5'-TTGCAT'TGCTGTCTCACAGGA-3'; GAPDH, forward: 5'-CTGGGCTACACTGAGCACC-3' and reverse: 5'-AAGTGGTCGTTGAGGGCAATG-3'.

Detection of Apoptosis

An annexin V-fluorescein isothiocyanate (FITC)/propidium iodide (PI) Apoptosis Detection Kit (A211-01, Vazyme, Nanjing, China) was utilized to assess HCCLM3-SR and Huh7-SR cell apoptosis. Specifically, 2×10^5 cells were digested with trypsin solution without ethylenediamine tetraacetic acid (EDTA) (GL0118, bjalb, Beijing, China) and centrifuged at 1000 rpm for 5 min at 4°C. After the removal of the supernatant, cells were subjected to two washes with phosphate-buffered saline (PBS, C10010500BT, IVDSHOW, Zhangjiakou, China) and centrifugation at 1000 rpm for 5 min at 4°C after each wash. Later, 100 μ L 1 \times Binding Buffer was used to re-suspend the cells, which were then incubated for 10 min with 5 μ L Annexin V-FITC and 5 μ L PI at room temperature, protected from light. Subsequently, 400 μ L 1 \times Binding Buffer was added. The cells were detected using the Attune NxT flow cytometry (DenLey, Guangzhou, China), and the apoptosis rate was calculated using FlowJo software (Becton Dickinson, SanJose, California, USA).

Determination of ROS Level

ROS level in HCCLM3, HCCLM3-SR, Huh7 and Huh7-SR cells was measured with 2',7'-Dichlorodihydrofluorescein diacetate (DCFH-DA) probe (HY-D0940, MedChemExpress, Monmouth Junction, USA) dissolved in DMSO. In brief, cells (1×10^4) were washed three times in Hanks' Balanced Salt Solution (HBSS, 3094984, Weibo, Guangzhou, China) after being inoculated into a 96-well plate. Cells were then subjected to 30-min incubation with 10 μ M DCFH-DA at 37°C, followed by analysis using the Attune NxT flow cytometry with FlowJo software.

Determination of Malondialdehyde Level

Malondialdehyde (MDA) level in Huh7, Huh7-SR, HCCLM3 and HCCLM3-SR cells was measured with a colorimetric kit (S0131S, Beyotime, Shanghai, China). Specifically, cells were given PBS at 4°C, lysed using RIPA lysis buffer (PH0316, Phygene, Fuzhou, China) and centrifuged at 10000 \times g for 10 min, followed by the collection of the supernatant. The samples were incubated for 15 min with MDA working solution (thiobarbituric acid (TBA) diluent, TBA storage solution and antioxidant) at 100°C. The samples were subjected to centrifugation at 1000 \times g for 10 min after cooling to the room temperature, followed by the collection of the supernatant. A microplate reader was used to measure the optical density value at 532 nm.

Thiobarbituric Acid Reactive Substances Assay

Thiobarbituric Acid Reactive Substances (TBARS) level in HCCLM3, HCCLM3-SR, Huh7 and Huh7-SR cells was detected with a TBARS Colorimetric Assay kit (E-BC-K298-M, Elabscience, Wuhan, China). Specifically, cells were given PBS at 4°C, lysed using RIPA lysis buffer and centrifuged at 10000 \times g for 10 min, followed by the collection of the supernatant. 0.1 mL standard or sample was added into corresponding 10 mL glass tubes. Each tube was added with 0.1 mL Clarificant and 4 mL chromogenic agent (Acid Reagent application solution and TBA Reagent application solution), followed by water bath for 1 h at 100°C. After cooling to the room temperature, centrifugation at 1600 \times g for 10 min was performed, and 0.25 mL supernatant was collected. A microplate reader was used to measure the optical density value at 532 nm.

Iron Assay

The ferrous iron (Fe^{2+}) level in HCCLM3, HCCLM3-SR, Huh7 and Huh7-SR cell lysates was determined using an iron assay kit (ab83366, Abcam, Cambridge, UK). Specifically, cells were given PBS at 4°C, lysed using RIPA lysis buffer and centrifuged at 10000 \times g for 10 min, followed by the collection of the supernatant. 100 μ L samples and standards were added to wells. 5 μ L Iron Reducer was added into each standard well, and 5 μ L assay buffer was added into each sample well, followed by 30-min incubation at 37°C. Later, each well was incubated with 100 μ L Iron Probe for 1 h at 37°C, protected from light. The output was measured using a microplate reader at 593 nm immediately.

Western Blot Analysis

Total proteins were extracted from HCCLM3, HCCLM3-SR, Huh7 and Huh7-SR cells using RIPA lysis buffer containing Halt Phosphatase Inhibitor Cocktail (78427, Thermo Fisher, Waltham, USA) and quantified by a BCA Protein Assay Kit (7780S, CST, Boston, Massachusetts, USA). Then equal quantities of proteins were loaded onto sodium dodecyl sulphate polyacrylamide gel electrophoresis (SDS-PAGE, SY0359, bjalb, Beijing, China) and transferred onto polyvinylidene difluoride (PVDF) membranes (88518, Thermo Fisher, Waltham, USA). After blocking with 5% non-fat milk for 2 h at room temperature, the membranes were incubated with primary antibody against solute carrier family 7 member 11 (SLC7A11, #12691, 35 kDa, 1:1000, CST, Boston, USA), glutathione peroxidase 4 (GPX4, #52455, 20 kDa, 1:1000, CST, Boston, USA), EFEMP1 (ab256457, 54 kDa, 1:1000, Abcam, Cambridge, UK), phosphorylated phosphoinositide 3-kinase (p-PI3K, ab278545, 84 kDa, 0.5 μ g/mL, Abcam, Cambridge, UK), phosphorylated protein-serine-threonine kinase (p-AKT, ab38449, 56 kDa, 1:1000, Abcam, Cambridge, UK) or the loading control GAPDH (ab8245, 37 kDa, 1:10000, Abcam, Cambridge, UK) overnight at 4°C. Subsequently, the membranes were washed in Tris-buffered saline with 0.1% Tween-20 (TBST, T854550-10EA, KE WEI CHEM, Shanghai, China) and incubated with Goat Anti-Rabbit IgG (AP132, 1:3000, Sigma-Aldrich, Saint Louis, USA) or Goat Anti-Mouse IgG (AP124, 1:3000, Sigma-Aldrich, Saint Louis, USA) for 1 h at room temperature. Finally, protein blots were detected using

Chemiluminescent Substrate (34577, Thermo Fisher, Waltham, USA) and the BioSpectrum Imaging System (Prime Science, Shanghai, China). The intensity of protein blots was analyzed using ImageJ software (National Institutes of Health, Bethesda, Maryland, USA).

Statistical Analysis

All quantitative results were expressed as mean \pm standard deviation. The differences between two groups were conducted by the independent sample *t* test. One-way analysis of variance was used to compare differences among multiple experimental groups. Graphpad 8.0 software was used for data analysis. Results with $P < 0.05$ were considered statistically significant.

RESULTS

IC50 of sorafenib was raised, and ROS/MDA/TBARS/ Fe^{2+} level was down-regulated in sorafenib-resistant HCC cells compared with those in normal HCC cells. HCCLM3, HCCLM3-SR, Huh7 and Huh7-SR cells were exposed for 24 h to sorafenib at 0, 4, 8, 16 or 32 μ M. Following the CCK-8 assay, the 24-h IC50 of sorafenib for HCCLM3, HCCLM3-SR, Huh7 and Huh7-SR cells was calculated. Following treatment with sorafenib at 8 or 16 μ M for 24 h, HCCLM3-SR cell viability was higher than HCCLM3 cell viability (Fig. 1A, $p < 0.05$). Following exposure to sorafenib at 4, 8, 16 or 32 μ M for 24 h, Huh7-SR cell viability was higher than sorafenib-sensitive Huh7 cell viability (Fig. 1A, $p < 0.001$). The IC50 of sorafenib for HCCLM3-SR and Huh7-SR cells was higher than that for HCCLM3 and Huh7 cells respectively (Fig. 1A, $P < 0.05$). HCCLM3, HCCLM3-SR, Huh7 and Huh7-SR cells received the same concentration (7 μ M) of sorafenib for 24 h. On sorafenib treatment, ROS level in HCCLM3-SR and Huh7-SR cells was lower than that in sorafenib-sensitive HCCLM3 and Huh7 cells respectively (Fig. 1B, $p < 0.001$). Compared with MDA level in sorafenib-sensitive HCCLM3 and Huh7 cells under sorafenib treatment, that in sorafenib-treated HCCLM3-SR and Huh7-SR cells was down-regulated respectively (Fig. 1C, $p < 0.01$). On sorafenib treatment, TBARS level in HCCLM3-SR and Huh7-SR cells was lower than that in HCCLM3 and Huh7 cells respectively (Fig. 1D, $p < 0.01$). Furthermore, Fe^{2+} level in sorafenib-treated HCCLM3-SR and Huh7-SR cells was lower than that in sorafenib-treated HCCLM3 and Huh7 cells respectively (Fig. 1E, $p < 0.05$). Taken together, IC50 of sorafenib was raised, and ROS, MDA, TBARS and Fe^{2+} levels were lowered in sorafenib-resistant HCC cells compared with those in normal HCC cells.

SLC7A11, GPX4, EFEMP1, p-AKT and p-PI3K were up-regulated in sorafenib-resistant HCC cells compared with those in normal HCC cells. On sorafenib treatment, SLC7A11 and GPX4 protein expressions in HCCLM3-SR and Huh7-SR cells were stronger than those in HCCLM3 and Huh7 cells respectively (Fig. 2A, $P < 0.001$). Under sorafenib treatment, EFEMP1, p-AKT and p-PI3K protein expression levels in HCCLM3-SR and Huh7-SR cells were higher than those in HCCLM3 and Huh7 cells respectively (Fig. 2B, $P < 0.001$). Accordingly, SLC7A11, GPX4, EFEMP1, p-AKT and p-PI3K were up-regulated in sorafenib-resistant HCC cells compared with those in normal HCC cells.

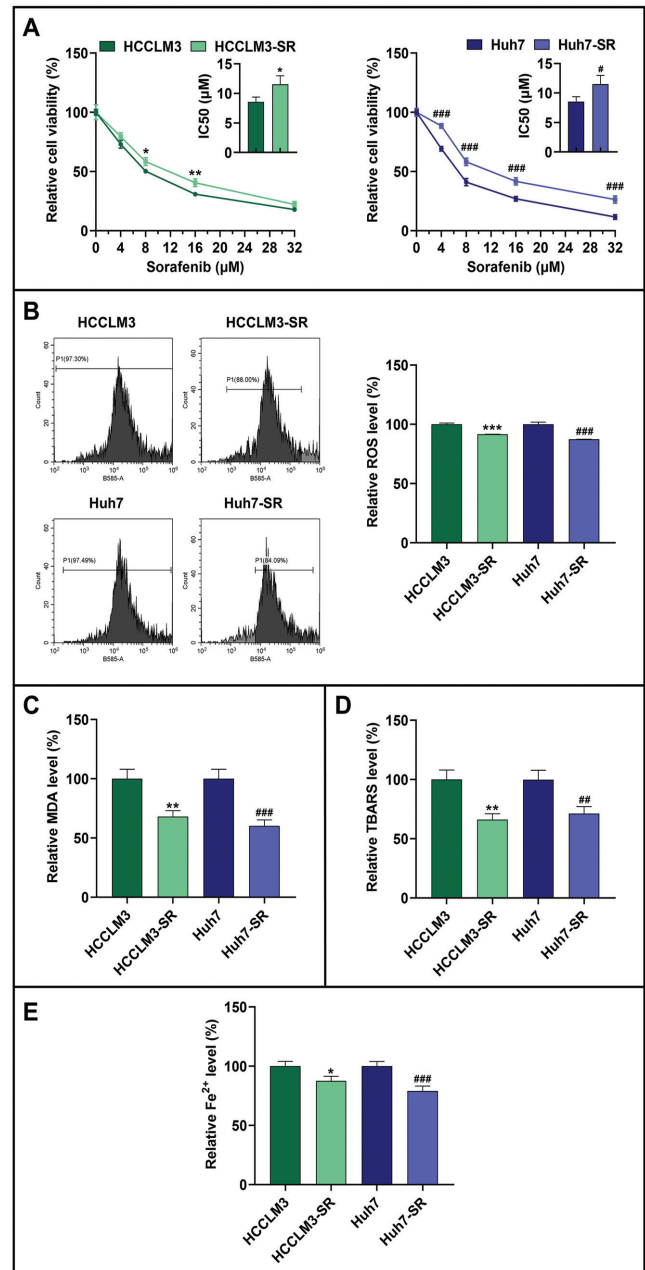


Fig. 1. IC50 of sorafenib was raised, and ROS, MDA, TBARS and Fe^{2+} levels were down-regulated in sorafenib-resistant HCC cells compared with those in normal HCC cells. (A) HCCLM3, HCCLM3-SR, Huh7 and Huh7-SR cells received sorafenib at 0, 4, 8, 16 or 32 μ M for 24 h. Viability of HCCLM3, HCCLM3-SR, Huh7 and Huh7-SR cells was detected and IC50 of sorafenib for these cells was calculated using CCK-8 assay. (B-E) HCCLM3, HCCLM3-SR, Huh7 and Huh7-SR cells were treated with sorafenib at 7 μ M for 24 h. (B) ROS level in HCCLM3, HCCLM3-SR, Huh7 and Huh7-SR cells was assessed by flow cytometry assay. (C) MDA level in HCCLM3, HCCLM3-SR, Huh7 and Huh7-SR cells was evaluated using colorimetry. (D) TBARS level in HCCLM3, HCCLM3-SR, Huh7 and Huh7-SR cells was detected by colorimetry. (E) Fe^{2+} level in HCCLM3, HCCLM3-SR, Huh7 and Huh7-SR cells was determined using colorimetry. * $p < 0.05$, ** $p < 0.01$, *** $p < 0.001$ vs. HCCLM3; # $p < 0.05$, ## $p < 0.01$, ### $p < 0.001$ vs. Huh7. (IC50: half-maximal drug inhibitory concentration; ROS: reactive oxygen species; MDA: malondialdehyde; TBARS: thiobarbituric acid reactive substances; Fe^{2+} : ferrous iron; HCC: hepatocellular carcinoma; HCCLM3-SR: sorafenib-resistant HCCLM3; CCK-8: Cell Counting Kit-8).

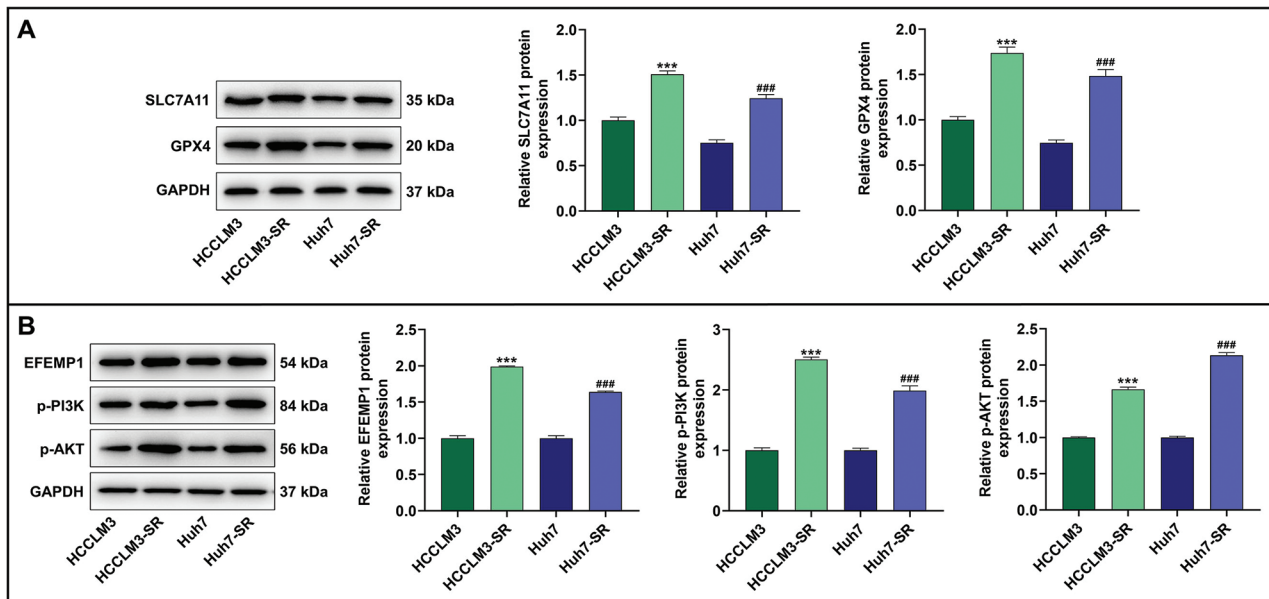


Fig. 2. SLC7A11, GPX4, EFEMP1, p-PI3K and p-AKT were up-regulated in sorafenib-resistant HCC cells compared with those in normal HCC cells. (A-B) HCCLM3, HCCLM3-SR, Huh7 and Huh7-SR cells were treated with sorafenib at 7 μ M for 24 h. (A) SLC7A11 and GPX4 protein expressions in HCCLM3, HCCLM3-SR, Huh7 and Huh7-SR cells were analyzed using Western blot with GAPDH used as a loading control. (B) EFEMP1, p-PI3K and p-AKT protein expressions in HCCLM3, HCCLM3-SR, Huh7 and Huh7-SR cells were detected by Western blot, and GAPDH was used as an internal standard. *** p <0.001 vs. HCCLM3; ### p <0.001 vs. Huh7. (SLC7A11: solute carrier family 7 member 11; GPX4: glutathione peroxidase 4; EFEMP1: epidermal growth factor-containing fibulin-like extracellular matrix protein 1; p-PI3K: phosphorylated phosphoinositide 3-kinase; p-AKT: phosphorylated protein-serine-threonine kinase; HCC: hepatocellular carcinoma; HCCLM3-SR: sorafenib-resistant HCCLM3).

EFEMP1 knockdown promoted apoptosis and up-regulated ROS, MDA, TBARS and Fe²⁺ levels in sorafenib-resistant HCC cells. ShEFEMP1 transfection markedly inhibited EFEMP1 mRNA expression in HCCLM3-SR and Huh7-SR cells (Fig. 3A, p <0.001). EFEMP1 knockdown promoted apoptosis of HCCLM3-SR and Huh7-SR cells under sorafenib treatment (Fig. 3B, p <0.001). ROS level in sorafenib-treated HCCLM3-SR and Huh7-SR cells was raised upon silencing EFEMP1 (Fig. 3C, p <0.001). EFEMP1 knockdown up-regulated MDA level in sorafenib-treated Huh7-SR and HCCLM3-SR cells (Fig. 3D, p <0.01). TBARS level in HCCLM3-SR and Huh7-SR cells under sorafenib treatment was up-regulated by knocking down EFEMP1 (Fig. 3E, p <0.01). EFEMP1 silencing raised Fe²⁺ level in sorafenib-treated HCCLM3-SR and Huh7-SR cells (Fig. 3F, p <0.001). Consequently, EFEMP1 silencing promoted apoptosis and up-regulated ROS, MDA, TBARS and Fe²⁺ levels in sorafenib-resistant HCC cells.

EFEMP1 silencing down-regulated SLC7A11, GPX4, p-AKT and p-PI3K in sorafenib-resistant HCC cells. EFEMP1 silencing repressed SLC7A11 and GPX4 protein expressions in HCCLM3-SR and Huh7-SR cells on sorafenib treatment (Fig. 4A, p <0.001). In addition, p-AKT and p-PI3K protein expression levels in sorafenib-treated Huh7-SR and HCCLM3-SR cells were down-regulated upon knocking down EFEMP1 (Fig. 4B, p <0.01). Therefore, EFEMP1 silencing down-regulated SLC7A11, GPX4, p-AKT and p-PI3K in sorafenib-resistant HCC cells.

DISCUSSION

An overwhelming majority of HCC cases are diagnosed at middle and late stages and are generally ineligible of hepatic resection and liver transplantation therapy, which leaves them relying heavily on the systematic treatment with TKIs [26]. The multi-targeted TKI sorafenib is the first targeted therapy for advanced HCC treatment [27], prolonging the survival time of patients. However, resistance to sorafenib develops to limit the drug efficacy [28].

Ferroptosis is a type of iron-dependent cell death that is morphologically, biochemically, and genetically different from apoptosis, necrosis, necroptosis and autophagy [29, 30]. Promoting ferroptosis augments the anti-cancer action of sorafenib in HCC [9]. Thus, it is imperative to understand the ferroptosis-related molecular mechanisms involved in sorafenib resistance in HCC. Ferroptosis is dependent on the elevation of lipid peroxidation driven by the Fenton reaction of Fe²⁺ [31]. Mechanically, iron is transferred through transferrin for endocytosis and then reduced by six-transmembrane epithelial antigen of the prostate 3 into Fe²⁺, which reacts with peroxides via Fenton reaction to yield a large amount of hydroxyl radicals, (a kind of ROS), whose accumulation results in lipid peroxidation [8, 32]. MDA is one of the final products of lipid peroxidation, and TBARS is a laboratory marker of oxidative stress, which can be utilized for the evaluation of lipid peroxidation [33-35]. Furthermore, SLC7A11 and GPX4 utilize glutathione to detoxify lipid peroxidation and play a crucial part in repressing ferroptosis [9, 36, 37].

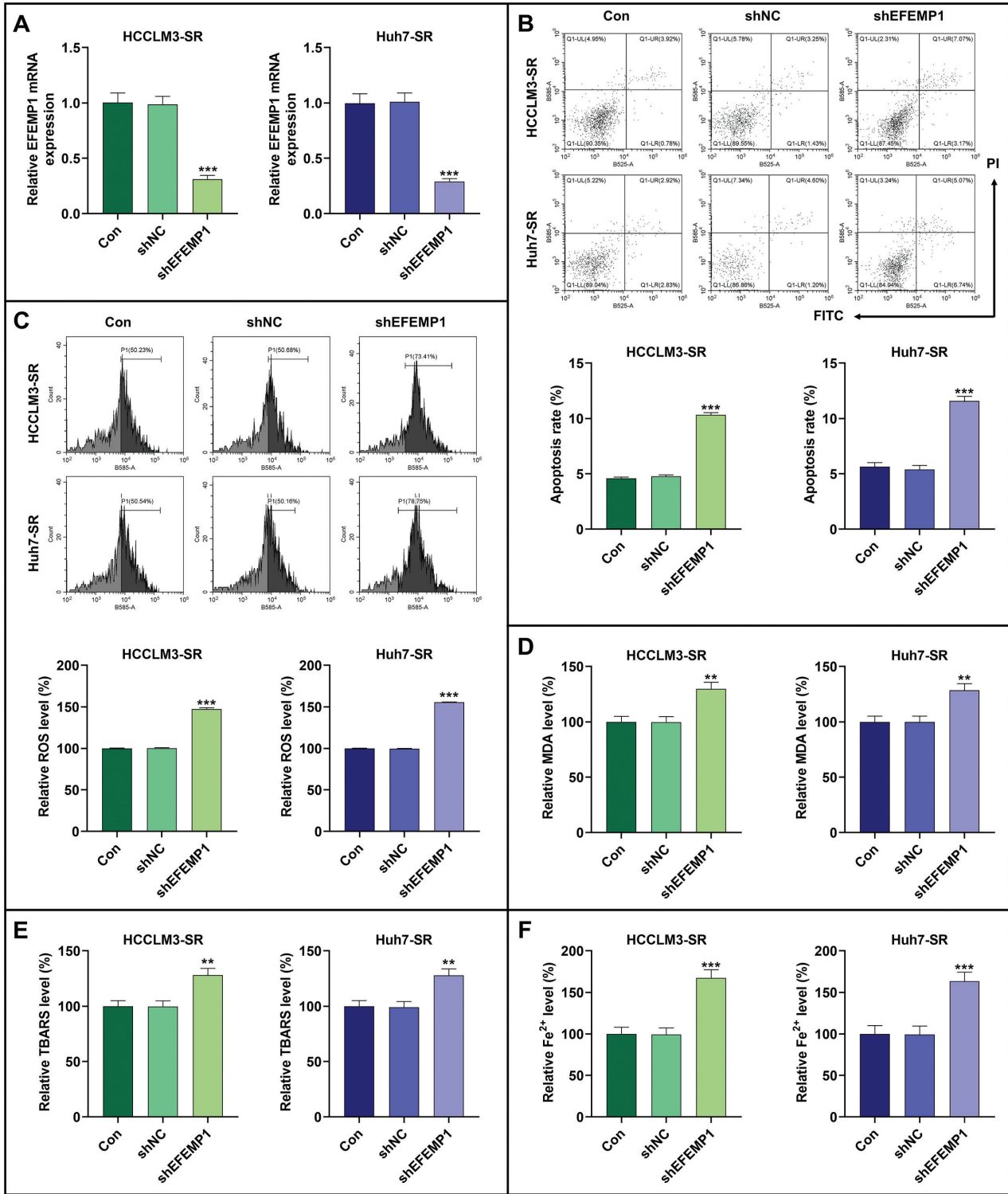


Fig. 3. EFEMP1 silencing promoted apoptosis and up-regulated ROS, MDA, TBARS and Fe²⁺ levels in sorafenib-resistant HCC cells (A) EFEMP1 mRNA expression in HCCLM3-SR and Huh7-SR cells transfected with shEFEMP1 or shNC or not was analyzed using qRT-PCR with GAPDH serving as a reference gene. (B-F) HCCLM3-SR and Huh7-SR cells were transfected with shEFEMP1 or shNC or not and treated with sorafenib at 7 μ M for 24 h. (B) HCCLM3-SR and Huh7-SR cell apoptosis was assessed by flow cytometry assay. (C) ROS level in HCCLM3-SR and Huh7-SR cells was detected by flow cytometry assay. (D) MDA level in HCCLM3-SR and Huh7-SR cells was evaluated using colorimetry. (E) TBARS level in HCCLM3-SR and Huh7-SR cells was detected by colorimetry. (F) Fe²⁺ level in HCCLM3-SR and Huh7-SR cells was determined using colorimetry. ***p*<0.01, ****p*<0.001 vs. shNC. (EFEMP1: epidermal growth factor-containing fibulin-like extracellular matrix protein 1; ROS: reactive oxygen species; MDA: malondialdehyde; TBARS: thiobarbituric acid reactive substances; Fe²⁺: ferrous iron; HCC: hepatocellular carcinoma; HCCLM3-SR: sorafenib-resistant HCCLM3; shEFEMP1: short hairpin RNA against EFEMP1; shNC: short hairpin RNA negative control; qRT-PCR: quantitative real time polymerase chain reaction; Con: control; PI: propidium iodide; FITC: fluorescein isothiocyanate).

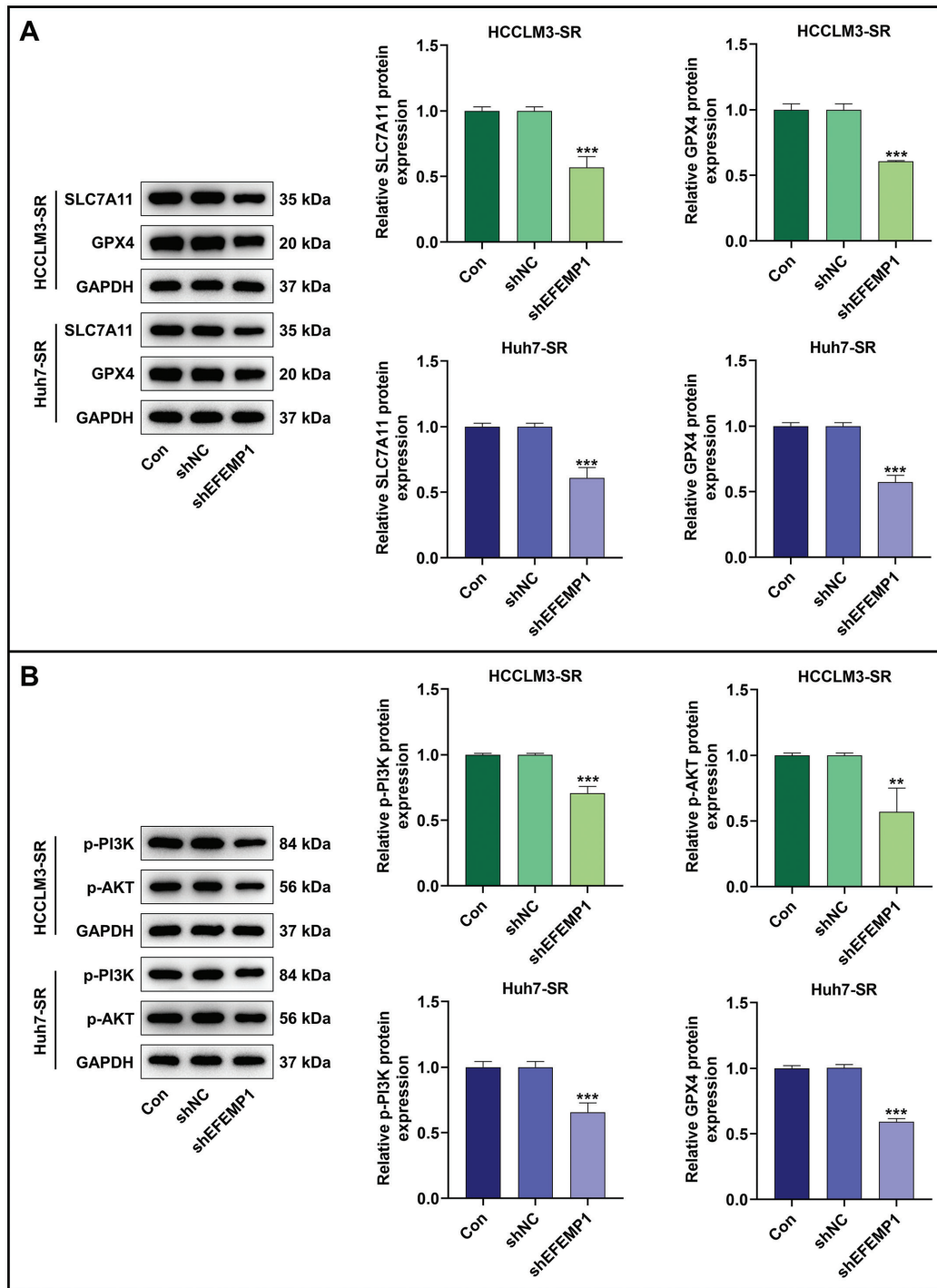


Fig. 4. EFEMP1 silencing down-regulated SLC7A11, GPX4, p-PI3K and p-AKT in sorafenib-resistant HCC cells. (A-B) HCCLM3-SR and Huh7-SR cells were transfected with shEFEMP1 or shNC or not and treated with sorafenib at 7 μ M for 24 h. (A) SLC7A11 and GPX4 protein expressions in HCCLM3-SR and Huh7-SR cells were analyzed using Western blot with GAPDH used as a loading control. (B) P-PI3K and p-AKT protein expressions in HCCLM3-SR and Huh7-SR cells were detected by Western blot, and GAPDH was used as an internal standard. ** $p < 0.01$, *** $p < 0.001$ vs. shNC. (EFEMP1: epidermal growth factor-containing fibulin-like extracellular matrix protein 1; SLC7A11: solute carrier family 7 member 11; GPX4: glutathione peroxidase 4; p-PI3K: phosphorylated phosphoinositide 3-kinase; p-AKT: phosphorylated protein-serine-threonine kinase; HCC: hepatocellular carcinoma; HCCLM3-SR: sorafenib-resistant HCCLM3; shEFEMP1: short hairpin RNA against EFEMP1; shNC: short hairpin RNA negative control; Con: control).

In this study, following sorafenib treatment, ROS, MDA, TBARS and Fe²⁺ contents in HCCLM3-SR and Huh7-SR cells were lower, and SLC7A11 and GPX4 expressions in HCCLM3-SR and Huh7-SR cells were stronger than those in HCCLM3 and Huh7 cells, indicating that ferroptosis is inhibited in

sorafenib-resistant HCC cells, which is in line with the previous report [10].

EFEMP1 exhibits antitumor or oncogenic activities towards human cancer, depending on the cancer type [18]. Previous research has portrayed EFEMP1 as a tumor suppressor low-

expressed in HCC [16, 17]. In contrast, we discovered EFEMP1 is up regulated in liver cancer cells exposed to sorafenib for a long period of time through bioinformatic analysis. Similarly, the findings of our *in-vitro* experiments reaffirmed that under sorafenib treatment, EFEMP1 expression in Huh7-SR and HCCLM3-SR cells was stronger than that in Huh7 and HCCLM3 cells. Nevertheless, the role of EFEMP1 in sorafenib-resistant HCC cells remains obscure. The induction of apoptosis, another type of regulated cell death, represents one important mechanism underlying the anti-cancer action of sorafenib [38]. Forced expression of EFEMP1 has been shown to induce the apoptosis of HCC cells [16]. On the contrary, under sorafenib treatment, EFEMP1 silencing promoted apoptosis of HCCLM3-SR and Huh7-SR cells, suggesting that EFEMP1 expression may contribute to the insensitivity of sorafenib-resistant HCC cells to sorafenib. Previous research has reported that EFEMP1 is required for the inhibition of ferroptosis by fibulin-1 in endometriosis [11]. In agreement with this role of EFEMP1 in endometriosis, our study found that under sorafenib treatment, EFEMP1 silencing up-regulated ROS, MDA, TBARS and Fe²⁺ levels and inhibited SLC7A11 and GPX4 expressions in HCCLM3-SR and Huh7-SR cells, therefore promoting the ferroptosis of sorafenib-resistant HCC cells. Given that augmenting ferroptosis enhance the effect of sorafenib against HCC [9], these findings suggested EFEMP1 knockdown promotes ferroptosis to overcome sorafenib resistance in HCC.

The PI3K/AKT pathway, a growth factor-regulated signaling, is aberrantly activated to reprogram cellular metabolism of cancer cells to benefit their malignant behaviors and thus promote the occurrence and progression of cancer [39]. Activating PI3K/AKT signaling facilitates the progression of HCC [20]. Inhibition of PI3K/AKT/mechanistic target of rapamycin (mTOR) signaling promotes apoptosis as well as autophagy (which can cause non-apoptotic cell death) of HCC cells [40]. The sorafenib resistance in HCC is enhanced via up-regulating the PI3K/AKT pathway [41], whereas suppressing PI3K/AKT/mTOR signaling inhibits the sorafenib resistance of HCC cells [42, 43] and increases the sorafenib sensitivity of sorafenib-resistant HCC [44]. Beyond this, PI3K/AKT/Nrf2 activation suppresses sorafenib-induced ferroptosis in sorafenib-resistant HCC cells to decrease the cells' sensitivity to sorafenib [22]. The enhanced phosphorylation of PI3K/AKT indicates PI3K/AKT activation [45]. Here, following sorafenib treatment, p-AKT and p-PI3K levels in HCCLM3-SR and Huh7-SR cells were higher than those in Huh7 and HCCLM3 cells, indicating an augmented PI3K/AKT activation in sorafenib-resistant HCC, which is consistent with the previous findings [22] and again hints its association with decreased sorafenib sensitive of sorafenib-resistant HCC. EFEMP1 has been reported to activate PI3K/AKT signaling to boost pleural mesothelioma growth [19]. Based on the above findings and the results obtained by us hereon, we surmised that knockdown of EFEMP1 enhances ferroptosis by mediating PI3K/AKT axis to restore the sensitivity of sorafenib-resistant HCC cells to sorafenib. The correctness of this surmise was later confirmed in our study through showing that EFEMP1 silencing inhibited p-AKT and p-PI3K expressions in HCCLM3-SR and Huh7-SR cells. The findings above unveiled that EFEMP1 silencing boosts ferroptosis by inactivating PI3K/AKT to overcome sorafenib resistance of HCC cells.

Our findings suggest promising translational avenues. Firstly, EFEMP1 could serve as a predictive biomarker to identify HCC patients at higher risk of developing sorafenib resistance. Previous proteomics and metabolomics analyses revealed that knocking down EFEMP1 significantly reduces drug resistance of liver cancer cells, indicating their potential as biomarkers for therapeutic response [46]. Secondly, therapeutic targeting of the EFEMP1/PI3K/AKT axis may overcome resistance. Previous studies have shown that the combination of CMG002 (a novel dual PI3K/mTOR inhibitor) and sorafenib significantly inhibits the proliferation of HCC cells and tumor formation by blocking the Ras/Raf/MAPK and PI3K/AKT/mTOR pathways [47]. Therefore, combining sorafenib with PI3K/AKT pathway inhibitors is a reasonable strategy. Third, promoting ferroptosis is a viable approach. Ferroptosis inducers (e.g., targeting SLC7A11 or GPX4) could be tested in combination with sorafenib, particularly for EFEMP1-high tumors. These strategies warrant further preclinical and clinical exploration.

Notwithstanding these potential applications, several limitations of the present study must be acknowledged. Firstly, the conclusions are drawn exclusively from *in vitro* experiments using two cell lines, necessitating further validation in animal models and clinical patient samples. Secondly, the precise mechanism by which EFEMP1 activates the PI3K/AKT pathway remains unclear and requires elucidation, further investigation into upstream regulators and direct binding partners of EFEMP1 in this context is needed. Thirdly, as a multifaceted ECM protein, EFEMP1 may influence sorafenib resistance through other mechanisms (e.g., epithelial-mesenchymal transition, tumor microenvironment), a more comprehensive analysis of its role is necessary. Finally, the potential involvement of other signaling pathways associated with EFEMP1, such as NF- κ B, was not explored.

CONCLUSIONS

To sum up, knockdown of EFEMP1 boosts ferroptosis via inactivating PI3K/AKT to resensitize sorafenib-resistant HCC to sorafenib, which suggests EFEMP1 as a target for sorafenib resistance in HCC. Nevertheless, more HCC cell lines need to be involved.

Conflicts of interest: None to declare.

Authors' contributions: T.Z. contributed to conceptualization and formal analysis. H.B.L. was involved in investigation and methodology. Y.M. participated in data curation and project administration. D.L.F. contributed to data curation. All authors were involved in writing the original draft and reviewing/editing the manuscript.

Acknowledgements: Funding: This research was supported by the Hangzhou Joint of the Zhejiang Provincial Natural Science Foundation of China under Grant NO.LHZY24H310003

REFERENCES

1. Gao R, Kalathur RKR, Coto-Llerena M, Ercan C, Buechel D, Shuang S, et al. YAP/TAZ and ATF4 drive resistance to Sorafenib in

- hepatocellular carcinoma by preventing ferroptosis. *EMBO Mol Med.* 2021;13(12):e14351. doi:10.15252/emmm.202114351
2. Lu Y, Chan YT, Tan HY, Zhang C, Guo W, Xu Y, et al. Epigenetic regulation of ferroptosis via ETS1/miR-23a-3p/ACSL4 axis mediates sorafenib resistance in human hepatocellular carcinoma. *J Exp Clin Cancer Res.* 2022;41(1):3. doi:10.1186/s13046-021-02208-x
 3. Xu J, Wan Z, Tang M, Lin Z, Jiang S, Ji L, et al. N(6)-methyladenosine-modified CircRNA-SORE sustains sorafenib resistance in hepatocellular carcinoma by regulating β -catenin signaling. *Mol Cancer.* 2020;19(1):163. doi:10.1186/s12943-020-01281-8
 4. Chidambaranathan-Reghupaty S, Fisher PB, Sarkar D. Hepatocellular carcinoma (HCC): Epidemiology, etiology and molecular classification. *Adv Cancer Res.* 2021;149:1-61. doi:10.1016/bs.acr.2020.10.001
 5. Connell LC, Harding JJ, Abou-Alfa GK. Advanced Hepatocellular Cancer: the Current State of Future Research. *Curr Treat Options Oncol.* 2016;17(8):43. doi:10.1007/s11864-016-0415-3
 6. Tang W, Chen Z, Zhang W, Cheng Y, Zhang B, Wu F, et al. The mechanisms of sorafenib resistance in hepatocellular carcinoma: theoretical basis and therapeutic aspects. *Signal Transduct Target Ther.* 2020;5(1):87. doi:10.1038/s41392-020-0187-x
 7. Liang Y. Mechanisms of sorafenib resistance in hepatocellular carcinoma. *Clin Res Hepatol Gastroenterol.* 2024;48(8):102434. doi:10.1016/j.clinre.2024.102434
 8. Li J, Cao F, Yin HL, Huang ZJ, Lin ZT, Mao N, et al. Ferroptosis: past, present and future. *Cell Death Dis.* 2020;11(2):88. doi:10.1038/s41419-020-2298-2
 9. Wang C, Cheng X, Peng H, Zhang Y. NIR-Triggered and ROS-Boosted NanoplatforM for Enhanced Chemo/PDT/PTT Synergistic Therapy of Sorafenib in Hepatocellular Carcinoma. *Nanoscale Res Lett.* 2022;17(1):92. doi:10.1186/s11671-022-03729-w
 10. Wan Y, Song Y, Chen J. Upregulated Fibulin-1 Increased Endometrial Stromal Cell Viability and Migration by Repressing EFEMP1-Dependent Ferroptosis in Endometriosis. *Oxid Med Cell Longev.* 2022;2022:4809415. doi:10.1155/2022/4809415
 11. de Vega S, Iwamoto T, Yamada Y. Fibulins: multiple roles in matrix structures and tissue functions. *Cell Mol Life Sci.* 2009;66(11-12):1890-902 doi:10.1007/s00018-009-8632-6
 12. Gallagher WM, Currid CA, Whelan LC. Fibulins and cancer: friend or foe? *Trends Mol Med.* 2005;11(7):336-40. doi:10.1016/j.molmed.2005.06.001
 13. Hu Y, Pioli PD, Siegel E, Zhang Q, Nelson J, Chaturvedi A, et al. EFEMP1 suppresses malignant glioma growth and exerts its action within the tumor extracellular compartment. *Mol Cancer.* 2011;10:123. doi:10.1186/1476-4598-10-123
 14. Hu B, Nandhu MS, Sim H, Agudelo-Garcia PA, Saldivar JC, Dolan CE, et al. Fibulin-3 promotes glioma growth and resistance through a novel paracrine regulation of Notch signaling. *Cancer Res.* 2012;72(15):3873-85. doi:10.1158/0008-5472.can-12-1060
 15. Hu J, Duan B, Jiang W, Fu S, Gao H, Lu L. Epidermal growth factor-containing fibulin-like extracellular matrix protein 1 (EFEMP1) suppressed the growth of hepatocellular carcinoma cells by promoting Semaphorin 3B(SEMA3B). *Cancer Med.* 2019;8(6):3152-66. doi:10.1002/cam4.2144
 16. Dou CY, Cao CJ, Wang Z, Zhang RH, Huang LL, Lian JY, et al. EFEMP1 inhibits migration of hepatocellular carcinoma by regulating MMP2 and MMP9 via ERK1/2 activity. *Oncol Rep.* 2016;35(6):3489-95. doi:10.3892/or.2016.4733
 17. Luo R, Zhang M, Liu L, Lu S, Zhang CZ, Yun J. Decrease of fibulin-3 in hepatocellular carcinoma indicates poor prognosis. *PLoS One.* 2013;8(8):e70511. doi:10.1371/journal.pone.0070511
 18. Roshini A, Goparaju C, Kundu S, Nandhu MS, Longo SL, Longo JA, et al. The extracellular matrix protein fibulin-3/EFEMP1 promotes pleural mesothelioma growth by activation of PI3K/Akt signaling. *Front Oncol.* 2022;12:1014749. doi:10.3389/fonc.2022.1014749
 19. Sun F, Wang J, Sun Q, Li F, Gao H, Xu L, et al. Interleukin-8 promotes integrin β 3 upregulation and cell invasion through PI3K/Akt pathway in hepatocellular carcinoma. *J Exp Clin Cancer Res.* 2019;38(1):449. doi:10.1186/s13046-019-1455-x
 20. Jiang H, Zhou Z. PRMT9 promotes hepatocellular carcinoma invasion and metastasis via activating PI3K/Akt/GSK-3 β /Snail signaling. *Cancer Sci.* 2018;109(5):1414-27. doi:10.1111/cas.13598
 21. Liu H, Zhao L, Wang M, Yang K, Jin Z, Zhao C, et al. FNDC5 Causes Resistance to Sorafenib by Activating the PI3K/Akt/Nrf2 Pathway in Hepatocellular Carcinoma Cells. *Front Oncol.* 2022;12:852095. doi:10.3389/fonc.2022.852095
 22. Lin Z, Xia S, Liang Y, Ji L, Pan Y, Jiang S, et al. LXR activation potentiates sorafenib sensitivity in HCC by activating microRNA-378a transcription. *Theranostics.* 2020;10(19):8834-50. doi:10.7150/thno.45158
 23. Xia S, Ji L, Tao L, Pan Y, Lin Z, Wan Z, et al. TAK1 Is a Novel Target in Hepatocellular Carcinoma and Contributes to Sorafenib Resistance. *Cell Mol Gastroenterol Hepatol.* 2021;12(3):1121-43. doi:10.1016/j.jcmgh.2021.04.016
 24. Chen C, Chen W, Li Y, Dong Y, Teng X, Nong Z, et al. Hyperbaric oxygen protects against myocardial reperfusion injury via the inhibition of inflammation and the modulation of autophagy. *Oncotarget.* 2017;8(67):111522-34. doi:10.18632/oncotarget.22869
 25. Chen Z, Yuan T, Yan F, Ye S, Xie Q, Zhang B, et al. CT-707 overcomes hypoxia-mediated sorafenib resistance in Hepatocellular carcinoma by inhibiting YAP signaling. *BMC Cancer.* 2022;22(1):425. doi:10.1186/s12885-022-09520-5
 26. Li B, Wei S, Yang L, Peng X, Ma Y, Wu B, et al. C1SD2 Promotes Resistance to Sorafenib-Induced Ferroptosis by Regulating Autophagy in Hepatocellular Carcinoma. *Front Oncol.* 2021;11:657723. doi:10.3389/fonc.2021.657723
 27. Gao L, Wang X, Tang Y, Huang S, Hu CA, Teng Y. FGF19/FGFR4 signaling contributes to the resistance of hepatocellular carcinoma to sorafenib. *J Exp Clin Cancer Res.* 2017;36(1):8. doi:10.1186/s13046-016-0478-9
 28. Dixon SJ, Lemberg KM, Lamprecht MR, Skouta R, Zaitsev EM, Gleason CE, et al. Ferroptosis: an iron-dependent form of nonapoptotic cell death. *Cell.* 2012;149(5):1060-72. doi:10.1016/j.cell.2012.03.042
 29. Stockwell BR. Ferroptosis turns 10: Emerging mechanisms, physiological functions, and therapeutic applications. *Cell.* 2022;185(14):2401-21. doi:10.1016/j.cell.2022.06.003
 30. Zhang Y, Ren X, Wang Y, Chen D, Jiang L, Li X, et al. Targeting Ferroptosis by Polydopamine Nanoparticles Protects Heart against Ischemia/Reperfusion Injury. *ACS Appl Mater Interfaces.* 2021;13(45):53671-82. doi:10.1021/acsami.1c18061
 31. Lei P, Bai T, Sun Y. Mechanisms of Ferroptosis and Relations With Regulated Cell Death: A Review. *Front Physiol.* 2019;10:139. doi:10.3389/fphys.2019.00139
 32. Zaki SM. Evaluation of antioxidant and anti-lipid peroxidation potentials of Nigella sativa and onion extract on nicotine-induced lung damage. *Folia Morphol.* 2019;78(3):554-63. doi:10.5603/FM.a2018.0117

33. Soares FAC, Filho NAK, Beretta BFS, Linden TS, Pöppel AG, González FHD. Thiobarbituric acid reactive substances in dogs with spontaneous hypercortisolism. *Domest Anim Endocrinol*. 2021;77:106634. doi:10.1016/j.domaniend.2021.106634
34. Aguilar Diaz De Leon J, Borges CR. Evaluation of Oxidative Stress in Biological Samples Using the Thiobarbituric Acid Reactive Substances Assay. *J Vis Exp*. 2020;(159). doi:10.3791/61122
35. Zhang F, Lei F, Xiao X. Knockdown of CBX7 inhibits ferroptosis in rats with cerebral ischemia and improves cognitive dysfunction by activating the Nrf2/HO-1 pathway. *J Biosci*. 2022;47. doi:10.1007/s12038-022-00307-2
36. Zhang Y, Swanda RV, Nie L. mTORC1 couples cyst(e)ine availability with GPX4 protein synthesis and ferroptosis regulation. *Nat Commun*. 2021;12(1):1589. doi:10.1038/s41467-021-21841-7
37. Hoxhaj G, Manning BD. The PI3K-AKT network at the interface of oncogenic signalling and cancer metabolism. *Nat Rev Cancer*. 2020;20(2):74-89. doi:10.1038/s41568-019-0216-7
38. Yang J, Pi C, Wang G. Inhibition of PI3K/Akt/mTOR pathway by apigenin induces apoptosis and autophagy in hepatocellular carcinoma cells. *Biomed Pharmacother*. 2018;103:699-707. doi:10.1016/j.biopha.2018.04.072
39. Xia P, Zhang H, Xu K, Jiang X, Gao M, Wang G, et al. MYC-targeted WDR4 promotes proliferation, metastasis, and sorafenib resistance by inducing CCNB1 translation in hepatocellular carcinoma. *Cell Death Dis*. 2021;12(7):691. doi:10.1038/s41419-021-03973-5
40. Liu T, Xie XL, Zhou X, Chen SX, Wang YJ, Shi LP, et al. Y-box binding protein 1 augments sorafenib resistance via the PI3K/Akt signaling pathway in hepatocellular carcinoma. *World J Gastroenterol*. 2021;27(28):4667-86. doi:10.3748/wjg.v27.i28.4667
41. Zhou X, Li TM, Luo JZ, Lan CL, Wei ZL, Fu TH, et al. CYP2C8 Suppress Proliferation, Migration, Invasion and Sorafenib Resistance of Hepatocellular Carcinoma via PI3K/Akt/p27(kip1) Axis. *J Hepatocell Carcinoma*. 2021;8:1323-38. doi:10.2147/jhc.s335425
42. Cao W, Liu X. BEZ235 Increases the Sensitivity of Hepatocellular Carcinoma to Sorafenib by Inhibiting PI3K/AKT/mTOR and Inducing Autophagy. *Oxid Med Cell Longev*. 2021;2021:5556306. doi:10.1155/2021/5556306
43. Lee J, Lim JW, Kim H. Astaxanthin Inhibits Matrix Metalloproteinase Expression by Suppressing PI3K/AKT/mTOR Activation in Helicobacter pylori-Infected Gastric Epithelial Cells. *Nutrients*. 2022;14(16):3417. doi:10.3390/nu14163417
44. Wang Z, Wu L, Zhou Y, Chen Z, Zhang T, Wei H, et al. Protein and metabolic profiles of tyrosine kinase inhibitors co-resistant liver cancer cells. *Front Pharmacol*. 2024;15:1394241. doi:10.3389/fphar.2024.1394241
45. Kim MN, Lee SM, Kim JS, Hwang SG. Preclinical efficacy of a novel dual PI3K/mTOR inhibitor, CMG002, alone and in combination with sorafenib in hepatocellular carcinoma. *Cancer Chemother Pharmacol*. 2019;84(4):809-17. doi:10.1007/s00280-019-03918-y